SN Computer Science (2026) 7:297
https://doi.org/10.1007/s42979-026-04875-z

ORIGINAL RESEARCH

Single-Camera Barbell Trajectory Analysis for the Snatch Lift

Dhairya Shah[1] · Hetav Raval[2] · Christopher Taber[5] · Tolga Kaya[4] · Eva Maddox[3] · Mehul S. Raval[1]

Received: 15 January 2026 / Accepted: 27 February 2026

Abstract

Olympic-style weightlifting requires a lot of coordination and complex motions, and keeping track of the barbell accurately is important for both performance evaluation and lowering the risk of injury. This work presents a single-camera, computer-vision framework that corrects for perspective distortion, automatically localizes the barbell using a YOLO-based detector, then tracks the barbell center with multiple 2D trackers, and finally applies a rule-based classifier to categorize snatch trajectories into four established types. The original rule-based classifier achieved 70% accuracy on a dataset of 10 competition snatch videos (about 6000 frames). The proposed YOLO initialization only changed the mean trajectory deviations by a few centimeters compared to manually initialized tracks, and the score category stayed the same for most lifts. Eight barbell kinematic variables are extracted, and three spatial measures–vertical peak height $Y_{\max}$, starting horizontal setup X_1, and bar drop Y_{drop}–are integrated into a 0–4 performance score matched to five qualitative categories from "Very Bad" to "Excellent." Sensitivity evaluations demonstrate that modest tracking noise and ±5–10% calibration perturbations infrequently affect the conformity of these kinematic variables to standard reference ranges, suggesting that the score is resilient to practical video and calibration inaccuracies. Further assessments of velocity, power, and tracker jitter quantify the correlation between dynamic barbell features and algorithmic decisions, as well as their influence on lift quality, yielding a more biomechanically interpretable and numerically reliable instrument for assessing applied snatch technique.

Keywords Computer vision · Deep learning · Injury risk prediction · Olympic weightlifting · Sports · Trajectory analysis

Dhairya Shah and Hetav Raval have contributed equally to this work.

✉ Hetav Raval
raval.het@northeastern.edu

Dhairya Shah
dhairya.s4@ahduni.edu.in

Christopher Taber
taberc@sacredheart.edu

Tolga Kaya
kayat@sacredheart.edu

Eva Maddox
emaddox@odu.edu

Mehul S. Raval
mehul.raval@ahduni.edu.in

[1] School of Engineering and Applied Science, Ahmedabad University, Navrangpura, Ahmedabad 380009, Gujarat, India

[2] Khoury College of Computer Sciences, Northeastern University, Fore Street, Portland 04101, Maine, USA

[3] School of Exercise Science, Old Dominion University, Hampton Blvd, Norfolk 23529, Virginia, USA

[4] School of Computer Science and Engineering, Sacred Heart University, Park Avenue, Fairfield 06825, Connecticut, USA

[5] Exercise Science, Sacred Heart University, Park Avenue, Fairfield 06825, Connecticut, USA

Published online: 24 March 2026

Introduction

Background

Weightlifting is a competitive strength sport featured in the Olympic Games, where athletes attempt to lift maximum weights in two highly technical lifts: the snatch and the clean and jerk. These lifts are not only demonstrations of pure power output but also demand exceptional strength, speed, flexibility, coordination, and balance. In the snatch, the athlete continuously lifts the barbell from the ground to an overhead position, requiring a wide grip and precise coordination to stabilize the weight overhead [1]. The clean and jerk is a two-phase lift; the 'clean' involves raising the barbell from the floor to the shoulders, followed by the 'jerk,' where the athlete propels the barbell overhead, typically using a split stance to catch and stabilize the weight [2]. Fig 1 shows both types of lifts: snatch, clean-and-jerk.

Each athlete is allowed three attempts in both the snatch and the clean and jerk. The best successful lift from each category is combined to form the athlete's total score. The athlete with the highest total in their weight class is ranked highest. In case of a tie, the lighter athlete is ranked higher [3]. Weight classes are divisions based on body mass, created to ensure fair competition among lifters of similar size. For example, as of the 2024 International Weightlifting Federation (IWF) classifications, men compete in 55 kg to 109+ kg, and women from 45 kg to 87+ kg [4]. These classes encourage inclusivity, structure competitions, and allow athletes of various body types to compete on a level playing field. While Olympic Weightlifting and Powerlifting are strength sports, Olympic weightlifting differs significantly from powerlifting. Olympic lifts emphasize explosive power, speed, flexibility, and technical precision, whereas powerlifting focuses more on maximum static strength in three lifts: squat, bench press, and deadlift [5].

A barbell is a long metal bar used in weight training and Olympic weightlifting, onto which varying weights (plates) are loaded. Standard Olympic barbells differ slightly between men's and women's categories. A men's barbell typically weighs 20 kg, measures 2.2 m long, and has a shaft diameter of 28 mm [8]. In contrast, a women's barbell weighs 15 kg, is 2.01 m long, and has a shaft diameter of 25 mm [8]. In the Olympics, the outer diameter of standard Olympic bumper plates is 45 cm, as defined by the IWF for all plates weighing 10 kg and above [9]. These plates are also color-coded for easy visual identification: red for 25 kg, blue for 20 kg, yellow for 15 kg, and green for 10 kg [10]. Accurate measurement of barbell trajectory in Olympic weightlifting is essential for optimizing technique, understanding movement patterns, and preventing injuries. Deviations from the ideal path can indicate mistimed pulls or poor positioning, leading to inefficient lifts or increased injury risk [11, 12].

(a) (i) (b) (ii)

Fig. 1 Lifts: i. A snatch being performed in competition [6], ii. A clean and jerk being performed in competition [7]

Olympic weightlifting movements, particularly the snatch, involve complex interactions between the athlete and the barbell, with subtle variations in force application and coordination significantly affecting performance outcomes. From a biomechanical perspective, the barbell trajectory serves as an indirect kinematic representation of the athlete–barbell system dynamics, reflecting how force is generated, transferred, and redirected across distinct movement phases. Prior biomechanics research indicates that an efficient snatch requires maintaining the barbell close to the athlete's base of support while achieving sufficient vertical displacement to enable rapid repositioning under the bar. Excessive horizontal deviations increase rotational moments about the lifter's center of mass, while unnecessary vertical displacement leads to higher energetic costs and reduced movement efficiency. Consequently, analyzing barbell trajectory provides a compact yet informative proxy for evaluating technical proficiency and identifying deviations from mechanically optimal lifting patterns.

Studying kinematics to analyze a weightlifter's performance and injury risk is crucial. Kinematics in weightlifting refers to the study of motion without considering the forces that drive it. It involves tracking the barbell and the lifter's body throughout the lift to assess performance. Key elements include the barbell trajectory (reflects movement efficiency and balance), joint angles (how well the athlete transitions through phases), body positioning (especially of the torso and hips for power generation), and the timing of movement phases (first pull, transition, second pull, and catch) [13, 14].

Biomechanical Basis for Barbell Trajectory Analysis

To formally contextualize the movement phases referenced in 1.1, the snatch lift is conventionally divided into distinct phases based on the barbell position and athlete posture [15]. (1) The first pull begins at lift-off and continues until the

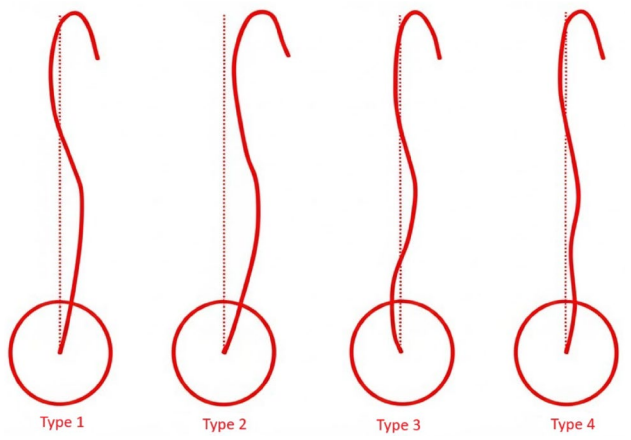

Fig. 2 Barbell trajectory types determined by the horizontal displacement pattern and vertical reference line crossing [18]

Table 1 Stable and variable biomechanical components of the snatch lift across movement phases (adapted from applied biomechanics literature)

Phase	Stable components	Variable components
Set position	Barbell positioned over mid-foot; balanced center of pressure	Hip height relative to knees; trunk inclination
First pull	Controlled vertical barbell displacement; constant trunk angle	Pull speed; knee extension timing
Transition	Barbell remains close to the body; re-bending of knees	Magnitude of horizontal displacement
Second pull	Coordinated triple extension; peak vertical acceleration	Peak barbell height achieved
Turnover	Active pull-under; minimal barbell drift	Arm path and elbow rotation strategy
Catch	Stable overhead fixation; barbell aligned with base of support	Depth of receiving position

barbell reaches approximately knee height, during which the lifter primarily elevates the bar while maintaining a relatively constant trunk angle. (2) The transition phase follows as the knees re-bend and the barbell is brought closer to the lifter's center of mass. (3) The second pull is characterized by rapid extension of the hips, knees, and ankles, producing the peak vertical acceleration of the barbell. (4) Finally, the catch phase occurs when the athlete actively pulls the barbell under and stabilizes it in the overhead position. These phase definitions provide a descriptive temporal structure of the lift. However, applied biomechanical analyses further examine how consistency and coordination across these phases contribute to efficient and repeatable lifting techniques.

Figure 2 shows the four types of barbell trajectories in the case of a snatch lift. Barbell trajectories are classified based on horizontal displacement relative to a vertical reference line [16]. Type 1 trajectory exhibits a "toward-away-toward" pattern, where the barbell initially moves toward the lifter, then away, and back toward the lifter, crossing the vertical reference line during the "away" phase. Type 2 trajectory also follows a "toward-away-toward" pattern but does not cross the vertical reference line at any point during the lift. Type 3 trajectory follows an "away-toward-away-toward" pattern, involving multiple crossings of the vertical reference line. Type 4 trajectory may begin with a "toward" phase, as in Type 1 or 2 trajectories, or an "away-toward" phase, as in the Type 3 trajectory. The defining feature of the Type 4 trajectory is an intervening "away-toward" phase between the first "toward" phase and the final "away-toward" phase.

While kinematic analysis provides a descriptive account of the barbell and body motion, its practical value in weightlifting is realized when these measurements are interpreted within an applied biomechanical framework. Such frameworks relate observable kinematic patterns to underlying technical objectives, allowing motion characteristics to be evaluated in terms of movement efficiency, load management, and performance consistency across athletes [17].

These stable components include maintaining the barbell close to the body during the pull, minimizing unnecessary horizontal displacement, and achieving coordinated vertical acceleration during the second pull. Previous applied studies further note that while elite lifters may exhibit stylistic variability, excessive deviations in barbell path are associated with increased joint loading and reduced lift success [15]. These biomechanical insights directly inform the selection of kinematic variables used in automated trajectory analysis systems, providing a principled basis for selecting and interpreting barbell motion metrics in relation to technical performance.

Applied biomechanical studies further distinguish between stable and variable components of the snatch technique across distinct movement phases. Stable components refer to movement characteristics consistently observed among technically proficient lifters, whereas variable components reflect individual adaptations arising from anthropometric differences and stylistic preferences [17]. Table 1 summarizes key stable and variable components reported in applied weightlifting biomechanics literature and provides context for interpreting barbell trajectory patterns.

These phase-specific stable components are commonly interpreted with respect to the athlete's base of support (BoS) and center of pressure (CoP), which serve as reference frames for evaluating barbell alignment and balance throughout the lift. Applied coaching frameworks emphasize maintaining the barbell trajectory within close proximity to the lifter's BoS to reduce excessive rotational moments and improve movement efficiency [17].

Within this biomechanical context, barbell trajectory patterns observed during the snatch have been

systematically classified based on their horizontal displacement characteristics.

Literature Review

Various methods have been used to analyze barbell trajectories, offering unique trade-offs in cost, accuracy, and practicality. Video-based analysis is among the most accessible techniques, relying on frame-by-frame tracking from standard or high-speed cameras [19, 20]. Motion capture systems using infrared cameras and reflective markers provide high-precision three-dimensional data but are expensive, require calibration, and are limited to laboratory environments [21]. Linear position and velocity transducers provide real-time data at high sampling rates, such as Tendo units [22] and GymAware [23]. However, they typically measure only vertical displacement and cannot capture horizontal or rotational movement [24]. Smartphone applications leverage onboard sensors or video algorithms to estimate barbell velocity and trajectory; they are highly accessible but generally lack the precision of dedicated systems [25]. Mathematical and computational modeling enables the simulation of barbell motion using kinematic and dynamic equations, providing insights into the forces and torques acting on the barbell. However, the models simplify assumptions that may not reflect actual lift conditions [26]. Wearable sensors and accelerometers provide portable, real-time feedback on barbell motion; however, they may be susceptible to noise and require careful calibration [27].

Traditional methods for assessing barbell trajectory typically involve manual video analysis, which can be subjective, labor-intensive, and prone to human error [20]. As a result, sports scientists have increasingly turned to automated approaches for motion analysis. Automation improves objectivity and reproducibility, offering high temporal resolution and reducing workload [28]. Computer vision techniques have emerged as particularly effective tools in this domain, enabling accurate motion tracking without the need for physical markers, which is ideal for minimally invasive performance assessment [29]. Markerless motion capture systems, powered by deep learning and pose estimation models, allow real-time analysis with reduced setup time and cost compared to traditional marker-based systems [30]. Despite these advances, most existing systems are sensitive to environmental variables and camera placement, limiting their generalization. In elite weightlifting, where minor technical differences can significantly impact performance, accurate analysis of barbell motion is essential. Studies at the 2015 World Weightlifting Championship and 2017 Pan-American Weightlifting Championship used standardized GoPro HERO4 Black camera setups to reduce measurement errors. Still, they did not account for variations in camera viewpoint, such as height and distance from the platform [18].

Given the above limitations, the paper develops a method to classify and track barbell trajectories independently of camera height and distance. The paper's contributions are: i. Creating a snatch lift video dataset and developing a barbell trajectory classification algorithm based on barbell movement. ii. A module to calculate the barbell kinematic variables from video analysis. iii. Suggest a metric based on kinematic variables for performance analysis. Also, compared to our previous work [31], this study presents an updated computer-vision framework for analyzing barbell trajectories in the snatch, linking trajectory patterns to biomechanical phases and lift quality. The improved system integrates automatic YOLO-based barbell detection, robust multi-tracker analysis, calibration sensitivity testing, and additional velocity/power metrics, evolving the work from a proof-of-concept into a more complete biomechanical assessment tool. The framework shows practical stability under realistic tracking noise and provides interpretable performance scoring grounded in kinematic behavior.

Methods

Participants

The participants were senior-level athletes, as defined by the International Weightlifting Federation and USA Weightlifting. The "Senior" age group comprises athletes aged 15 and older, with no upper age limit until the "Masters" category begins at 35. The dataset was collected during a local competition in the United States, an open-access meet. These are entry-level events, often organized by clubs or regional associations. They are accessible to a wide range of lifters, including beginners and experienced athletes. A total of 44 athletes participated in the study, comprising 28 males (mean body weight = 89.88 kg) and 16 females (mean body weight = 73.27 kg). In this paper, a random sample of the collected dataset was used for analysis. This study was approved by the Sacred Heart University Institutional Review Board, approval number IRB-FY2025-241, in April 2025.

Data Acquisition and Annotation

The data were collected during the East Coast Gold Spring Fling, a USA Weightlifting-sanctioned regional meet, on April 12, 2025, in Virginia Beach, Virginia, USA. A GoPro HERO10 Black action camera was employed for video acquisition due to its compact design, image stabilization, and high-resolution recording capabilities. The HERO10

(a) (i) (b) (ii) (c) (iii)

Fig. 3 Sample data frames from the video dataset: i. Athlete starting the lift, ii. Athlete in the middle of the lift, iii. The athlete finished the lift

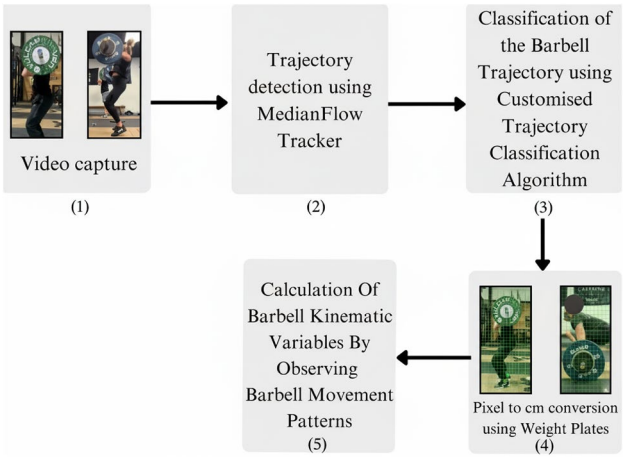

Fig. 4 The flow for video processing and calculation of barbell kinematic variables

features a 23MP sensor and supports video capture up to 5K at 30 frames per second (fps) or 4K at 60 fps, enabling detailed analysis of fast barbell movements [32]. The camera was placed at 3.35 m from the barbell, and the videos were recorded at 2160p resolution. A controlled environment was established to minimize external factors affecting data quality. Subsequently, the weightlifter recorded a series of snatch lift attempts. The data were collected, ensuring a diverse sample across weight categories and skill levels. The data included over 200 trials, comprising more than 100,000 video frames captured from various angles, distances, and heights. Some sample frames are shown in Fig. 3. Our study requires camera placement in a lateral plane aligned with the barbell axis, and 10 videos from the dataset have been selected accordingly. An expert labeled each sample video as Types 1-4 based on the trajectory.

In this work, the barbell trajectory is modeled as a two-dimensional discrete-time signal extracted from monocular video data. Let the trajectory be defined as $T = \{(x_t, y_t)\}_{t=1}^{N}$, where x_t and y_t represent the horizontal and vertical pixel coordinates of the barbell center at frame t, and N denotes the total number of frames corresponding to a single lift. This representation enables the direct application of signal-processing techniques for analyzing kinematic patterns over time. However, trajectories extracted from video are subject to several sources of noise, including camera jitter, motion blur during high-velocity phases, tracking drift, and perspective distortion inherent to monocular viewpoints. These factors motivate the use of relative, displacement measures normalized by the athlete's height rather than absolute positional values when computing kinematic descriptors.

Video Processing and Frame Extraction

Figure 4 illustrates the overall workflow for video processing and barbell trajectory detection. After collecting the data, the videos were resized to (1920×1080) to standardize the dataset's width and height. Videos were trimmed at the start and end to include only the lift's motion, thereby avoiding redundant frames. After that, the MedianFlow tracking algorithm [33] was deployed to track the movement of the snatch lift performed by the athlete. MedianFlow operates by monitoring a set of points using forward-backward error estimation. It first estimates the trajectory of each point from frame to frame, then validates tracking consistency by comparing forward and backward paths and filtering out unreliable points. This makes the algorithm robust to partial occlusions and abrupt motions. The extracted coordinates obtained by tracking the snatch lift were stored in a CSV file, which we used to compute kinematic variables of the snatch lift.

Automated Barbell Detection and Tracking

In our previous work [31], the barbell was localized manually in the first frame before initializing MedianFlow tracking [18]. In this extended work, we replaced manual initialization with an automatic detector based on YOLOv11n [34]. The detector is trained on labeled frames

extracted from the same ten competition videos used in this study, where the barbell plates are annotated with axis-aligned bounding boxes. During inference, YOLOv11n predicts a bounding box around the barbell; the center of this box defines the initial tracking point. Detections with confidence below τ_{det} are discarded, and non-maximum suppression with IoU threshold τ_{iou} is applied to remove duplicate boxes. The highest-confidence box after suppression is used to initialize the tracker.

In our earlier work [31], the barbell center was tracked using the MedianFlow tracker in OpenCV [35]. In this extended study, we further utilized Kernelized Correlation Filters (KCF) and Dlib tracker on the same ten videos. For each tracker, we initialize from the YOLO detection in the first frame and run frame-by-frame tracking to obtain (x_t, y_t). A track is marked as a failure if the bounding box leaves the image, collapses below a minimum size, or if the built-in tracker flag indicates loss. To quantify positional jitter, we compute the frame-to-frame standard deviation of the barbell center after smoothing, and we propagate each tracker's coordinates through the kinematic and scoring pipeline.

To quantify the accuracy of YOLO-based trajectories, we compared them against trajectories obtained from manual barbell centre initialization. For each video, let $(x_t^{\text{man}}, y_t^{\text{man}})$ and $(x_t^{\text{yolo}}, y_t^{\text{yolo}})$ denote the calibrated barbell centre coordinates at frame t (in cm) for the manual and YOLOv11n pipelines, respectively. The per-frame position error is

$$e_t = \sqrt{\left(x_t^{\text{yolo}} - x_t^{\text{man}}\right)^2 + \left(y_t^{\text{yolo}} - y_t^{\text{man}}\right)^2}. \quad (1)$$

For each lift, we report the mean, median, and maximum of e_t across all valid frames. In addition, both trajectories are passed through the kinematic and scoring pipeline to obtain $Y_{\max}$, X_1, Y_{drop}, trajectory type, and the 0–4 performance score, allowing us to count how often YOLO-based tracking changes any of these outputs.

Calibration: Pixel to Centimeter Mapping Using Weight Plates

Initially represented in pixels, the coordinates extracted from the CSV file were converted to centimeters to ensure consistency with real-world distance measurements. This transformation was essential for meaningful biomechanical analysis, as kinematic variables such as displacement, velocity, and acceleration must be expressed in physical units to interpret athlete performance and assess potential injury risks [36].

To achieve this, a known reference object, the weight plate attached to the barbell, was used for calibration. A pixel-to-centimeter conversion factor was calculated by identifying the number of pixels corresponding to the visible plate diameter in the video frame.

Barbell Trajectory Classification

The study on barbell trajectory distribution varies across weight categories. The most common trajectory was Type 3, observed in 53% of lifters at the 2015 World Weightlifting Championships (WWC) and 59% at the 2017 Pan-American Weightlifting Championships (PAWC) [18]. It was particularly prevalent among heavier male lifters and top finishers. Type 2, which does not cross the vertical reference line, was the second most frequent, representing about 30% of male and female lifters. In contrast, Type 1 was less common, occurring in 13% of lifts at WWC and 8% at PAWC. The rarest trajectory was Type 4, accounting for just 6% at WWC and 3% at PAWC, respectively.

A machine learning (ML) approach was not employed due to a lack of a large dataset, causing data imbalance and bias. As a result, we adopted a rule-based approach, analyzing horizontal displacement patterns to classify barbell trajectories and determine whether the barbell crosses the

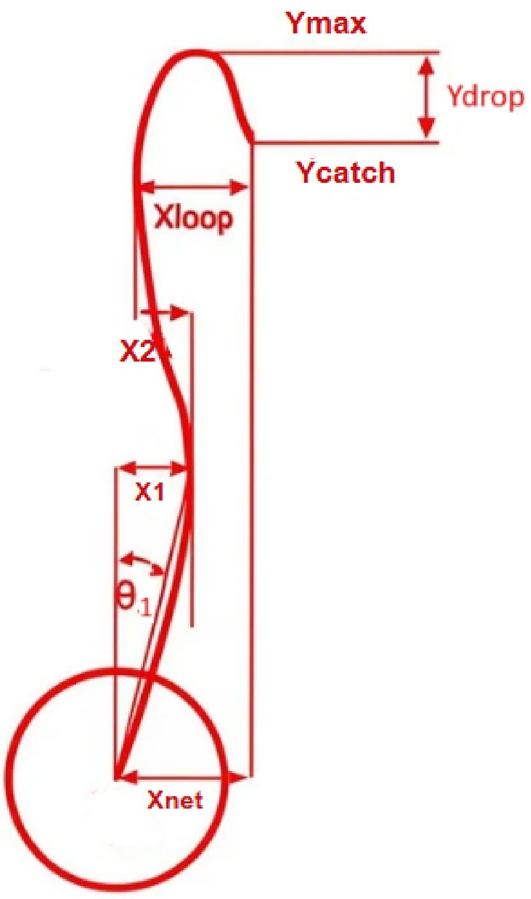

Fig. 5 Barbell kinematic variables of displacement [18]

vertical reference line at critical points. The classification is based on key motion parameters extracted from tracking data and described by Algorithm 1. If no matching type is found, the algorithm adds them to the “unknown" category for review.

Calculation of Barbell Kinematic Variables

Eight key barbell kinematic variables are associated with the snatch lift as shown in Fig. 5. These variables help us determine whether the lift was performed accurately or posed an

Require: Standardized barbell trajectory coordinates $C = [(x_1, y_1), (x_2, y_2), \ldots, (x_n, y_n)]$
Ensure: Classified trajectory type

$x\_negative \leftarrow$ `false` ▷ Tracks if x becomes negative
$x\_cycles \leftarrow 0$ ▷ Counts oscillations in x direction
$increasing\_y \leftarrow$ `true` ▷ Tracks if y is increasing
$phase \leftarrow$ `increasing` ▷ Current trend of x
for $i \leftarrow 2$ **to** n **do**
  $x \leftarrow x_i$
  $y \leftarrow y_i$
  if $x < 0$ **then**
    ▷ Check if any previous x_k was positive
    if no $k \in \{1, \ldots, i\}$ such that $x_k > 0$ **then**
      return Trajectory Type 3
    end if
    $x\_negative \leftarrow$ `true`
  end if
  if $i > 2$ **and** $y < y_{i-1}$ **then**
    $increasing\_y \leftarrow$ `false`
  end if
  if $increasing\_y$ **then**
    $prev\_x \leftarrow x_{i-1}$
    if $phase =$ `increasing` **and** $x < prev\_x$ **then**
      $phase \leftarrow$ `decreasing`
    else if $phase =$ `decreasing` **and** $x > prev\_x$ **then**
      $x\_cycles \leftarrow x\_cycles + 1$
      $phase \leftarrow$ `increasing`
    end if
  end if
end for
if not $x\_negative$ **then**
  return Trajectory Type 2
else if $x\_cycles \geq 2$ **then**
  return Trajectory Type 4
else if $x\_cycles = 1$ **then**
  return Trajectory Type 1
else
  return No matching trajectory type detected
end if

Algorithm 1 Barbell trajectory classification

injury risk. We consider the center of the barbell rod to be the origin of our analysis. The eight kinematic parameters are discussed as follows:

1) $Y_{\max}$

It is the highest point achieved during the lift [18], calculated as the highest y-coordinate during the lift.

2) Y_{catch}

It is the height of the catch [18], calculated by finding the lowest y-coordinate post $Y_{\max}$, which happens due to the load of the weight of the barbell before the y-coordinate starts increasing again.

3) Y_{drop}

It is the difference between $Y_{\max}$ and Y_{catch} [18], measured by the difference of y-coordinates of $Y_{\max}$ and Y_{catch}. The less the Y_{drop}, the better the athlete has performed the lift and the lower the chances of injury.

4) X_{net}

It is the net horizontal displacement from the start position to Y_{catch} [18]. Since the origin is at (0,0), X_{net} is simply the x-coordinate of Y_{catch}:

$$X_{\text{net}} = x_{\text{catch}} \tag{2}$$

5) X_1

It is the net horizontal displacement from the start to the most rearward position during the first displacement phase toward the lifter [18]. To calculate X_1, we ignore all the negative x-coordinates until the x-coordinate starts increasing. X_1 is the maximum value before the x-coordinates start decreasing.

6) θ_1

It is the angle relative to the vertical reference line from the start position to the position at X_1 [18]. It is calculated as:

$$\theta_1 = \tan^{-1}\left(\frac{X_1}{y_{\text{X1}}}\right) \tag{3}$$

where y_{X1} is the y-coordinate corresponding to X_1.

7) X_2

It is the horizontal distance from X_1 to the most anterior position between X_1 and $Y_{\max}$ [18]. Since the x-coordinates start decreasing after X_1, we define a temporary coordinate x_{temp} as the minimum value before x-coordinates start increasing again. Then, X_2 is calculated as:

$$X_2 = X_1 - x_{\text{temp}} \tag{4}$$

8) X_{loop}

It is the horizontal distance from X_2 to Y_{catch} [18]. It is given by:

$$X_{\text{loop}} = x_{\text{catch}} - x_{\text{temp}} \tag{5}$$

Table 2 Mapping of extracted kinematic features to snatch phases and biomechanical interpretation

Feature	Primary phase	Biomechanical interpretation	Coaching cue
X_1	Set/first pull	Initial barbell alignment relative to the base of support reflects the setup consistency and balance at lift-off	Adjust set position; keep bar over mid-foot
Y_{max}	Second pull	Vertical impulse generated through coordinated triple extension	Emphasize powerful hip extension
Y_{drop}	Turnover/catch	Efficiency of pull-under and speed of barbell fixation overhead	Faster transition under the bar
X_{net}	Entire lift	Cumulative horizontal deviation indicating trajectory efficiency	Keep bar path close to the body

The selected kinematic features are designed to capture biomechanically meaningful aspects of snatch technique across distinct movement phases. The maximum vertical displacement Y_{max} reflects the effectiveness of force production during the second pull, while the vertical drop distance Y_{drop} provides insight into the efficiency of the turnover and the athlete's ability to reposition under the barbell. Horizontal displacement measures such as X_1 and net horizontal displacement X_{net} characterize the barbell's proximity to the lifter's base of support and quantify cumulative horizontal deviation throughout the lift. To facilitate comparison across athletes with differing anthropometry, all vertical displacement measures were normalized by athlete height, preserving biomechanical relevance while reducing inter-subject variability.

To establish a direct connection between extracted kinematic variables and applied biomechanical principles, each feature can be associated with a specific phase of the

snatch and its underlying technical objective as shown in Table 2. This mapping enables the interpretation of numerical deviations in terms of phase-wise technical execution, as commonly used in applied weightlifting analysis. Applied biomechanical analyses of Olympic weightlifting emphasize that technical errors often manifest in a phase-specific manner and can be inferred from barbell trajectory characteristics. During the set and first pull, improper barbell alignment relative to the base of support may result in early horizontal drift, reflected by elevated initial displacement values. Errors during the transition phase, such as delayed knee re-bend or loss of bar proximity, often introduce oscillatory horizontal motion. Inefficient execution of the second pull typically results in reduced peak vertical displacement, indicating insufficient vertical impulse. Finally, delays or inefficiencies during the turnover and catch phases are commonly associated with increased vertical drop distances, reflecting slower repositioning of the athlete beneath the barbell. This phase-wise interpretation framework as shown in Table 2 provides biomechanical context for diagnosing technique deficiencies using trajectory-derived kinematic features.

Calibration Sensitivity Analysis for Kinematics Parameters

To assess how sensitive the derived kinematic variables are to calibration errors, we systematically perturbed the pixel-to-centimetre scale factor. Let s denote the nominal scale (cm per pixel). For each lift we generated perturbed scales $s' \in \{0.90s, 0.95s, 1.05s, 1.10s\}$, corresponding to $\pm 5\%$ and $\pm 10\%$ calibration errors. The full barbell trajectory was recomputed under each s', and the resulting $Y_{\max}$, X_1, Y_{drop}, trajectory type, and 0–4 performance scores were recalculated. We then counted, for each level of perturbation, how often the in-range/out-of-range status of each variable changed and how often the overall performance score changed. The described procedure is a straightforward sensitivity analysis of simulated calibration error in the pixel-to-centimeter scale and provides a robustness analysis of kinematic metrics under scale-factor perturbations.

Table 3 Assigning categories to the score value

Score value	Interpretation	Score category
0	Incorrect trajectory	Very bad
1	Correct trajectory, but all parameters outside range	Bad
2	Correct trajectory, but two parameters outside range	Fair
3	Correct trajectory, but one parameter outside range	Good
4	Correct trajectory and all parameters within range	Excellent

Athlete Performance Scoring

To properly validate our method, we needed a way to measure performance after correct trajectory classification. Therefore, we measure three barbell kinematic parameters: Y_{max}, X_1, and Y_{drop} to generate a score for the lifting performance. Here, Y_{max} shows how much vertical height the athlete generated [16], X_1 indicates the initial barbell balance and setup [37], and Y_{drop} relates to how efficiently the athlete transitions into the catch phase [38].

For each repetition, an athlete receives a performance score from 0 to 4 based on trajectory classification and three kinematic parameters. A score of 1 is given for a correctly classified trajectory, and up to 3 additional points (1 for each parameter) are awarded if the corresponding kinematic values fall within the typical ranges reported for Olympic weightlifting. If the trajectory is misclassified, the score is 0, and no kinematic checks are performed. Thus, 0 indicates an incorrect trajectory, while 4 indicates a correct trajectory with all kinematic parameters within the expected range, and each score from 0 to 4 is further mapped to one of five qualitative categories from "very bad" to "excellent.", as shown in Table 3.

Peak Velocity and Power Computation

In order to correlate scores and peak power, from the calibrated barbell coordinates (x_t, y_t) (cm) sampled at frame rate f (Hz), we compute horizontal and vertical velocities using central finite differences:

$$v_x(t) = \frac{x_{t+1} - x_{t-1}}{2/f}, \qquad v_y(t) = \frac{y_{t+1} - y_{t-1}}{2/f}. \tag{6}$$

Vertical acceleration is obtained as

$$a_y(t) = \frac{v_y(t+1) - v_y(t-1)}{2/f}. \tag{7}$$

Given barbell mass m_{bar}, instantaneous barbell power is

$$P(t) = m_{\text{bar}} \left(a_y(t) + g\right) v_y(t), \tag{8}$$

where g is gravitational acceleration. From these time series, we extracted peak vertical force, peak velocity, and peak power within the pull phases, and reported them both in absolute values.

Table 4 YOLO barbell detection performance (mAP@50-95) for different camera views

View subset	# Images	mAP@50-95(%)	mAP@50(%)
Ten lateral videos	150	50.7	94.7
Slightly oblique videos	50	39.4	82.0
Highly oblique videos	50	29.4	72.0

Oblique views show reduced accuracy compared with near-lateral footage

Results and Discussion

Our investigation analyzed the barbell trajectories during athletes' weightlifting sessions across 6000 frames from 10 videos.

Automatic Barbell Detection Performance

Table 4 summarizes the detection performance of the YOLOv11 barbell detector across three camera view categories. Intersection over Union (IoU) is a localization metric used for detection. It quantifies the overlap between a predicted bounding box and its corresponding ground-truth box as the ratio of their intersection area to their union area, with values ranging from 0 (no overlap) to 1 (perfect overlap). A prediction is considered a correct detection if its IoU with a ground-truth box exceeds a specified threshold. IoU is used alongside Mean Average Precision at IoU 0.5 (mAP@50), which evaluates detection performance using a single, relatively lenient IoU threshold of 0.5, computing Average Precision (area under the precision–recall curve) per class and then averaging across all classes. In contrast, mAP@50–95 (often denoted mAP@0.5:0.95) averages the AP over multiple IoU thresholds from 0.50 to 0.95 in steps of 0.05, providing a stricter measure that jointly reflects both detection capability and bounding-box localization accuracy.

On near-lateral footage—the intended use case for the system—the detector achieved an mAP@50 of 94.7% and mAP@50-95 of 50.7%, indicating robust detection with high overlap between predicted and ground-truth bounding boxes. As the camera angle deviated from lateral, performance degraded progressively: slightly oblique videos yielded mAP@50 of 82.0% (mAP@50-95: 39.4%), while highly oblique footage dropped to mAP@50 of 72.0% (mAP@50-95: 29.4%).

Figure 6 illustrates this degradation qualitatively. In lateral views (panel a), the detector produces tight bounding boxes centered accurately on the barbell plates, yielding IoU values exceeding 0.9. At slight oblique angles (panel b), detections remain usable but exhibit minor misalignment, with IoU dropping to approximately 0.78. Highly oblique views (panel c) pose the greatest challenges: the elliptical appearance of the plates at non-perpendicular angles, combined with potential occlusion by the athlete's body, causes bounding boxes to shift or expand inappropriately, resulting in an IoU of 0.54 or lower.

These results have practical implications for deployment. The 22.7 percentage-point drop in mAP@50 from lateral to highly oblique views (94.7% to 72.0%) indicates that camera placement is a critical factor in system reliability. For competition or training environments where near-lateral positioning is feasible, the detector provides sufficient accuracy for automatic trajectory initialization. However, in constrained settings where only oblique footage is available, manual region-of-interest (ROI) selection may remain preferable to avoid propagating initialization errors into the subsequent tracking phase. The periodic YOLO re-detection mechanism (every 30 frames) helps mitigate drift in such cases, but cannot fully compensate for systematic localization bias introduced by poor viewing angles.

Tracker Solution for Barbell Trajectory Detection

We experimented with different trackers to detect the barbell trajectory, including Boosting, MIL (Multiple Instance Learning), KCF (Kernelised Correlation Filters), TLD (Tracking-Learning-Detection), MedianFlow, GoTurn, DlibTracker, CamShift, and Template Matching. In our study, we recorded videos directly in the athlete's lateral plane, introducing challenges such as background clutter and potential occlusions due to static objects in the environment.

Among the trackers evaluated, the MedianFlow tracker consistently provided the most accurate and stable

(a) Lateral view (b) Slightly oblique view (c) Highly oblique view

Fig. 6 Effect of camera angle on YOLO barbell detection quality

Table 5 Tracker performance with manual ROI initialization

Tracker	Failure rate (%)	Jitter (cm)	Type Diff. (%)	Score Diff. (%)
MedianFlow	0.00 ± 0.00	0.776 ± 0.211	–	–
KCF	82.18 ± 6.80	0.070 ± 0.067	40.0	86.0
Dlib tracker	3.59 ± 5.95	0.793 ± 0.187	40.0	30.0

MedianFlow serves as the baseline for comparing trajectory types and scores

Table 6 Tracker performance with YOLOv11 auto-detection and periodic re-initialization every 30 frames

Tracker	Failure rate (%)	Jitter (cm)	Type Diff. (%)	Score Diff. (%)
MedianFlow	0.00 ± 0.00	0.774 ± 0.209	–	–
KCF	38.79 ± 18.74	0.750 ± 0.189	20.0	40.0
Dlib tracker	0.52 ± 0.91	0.813 ± 0.190	30.0	30.0

MedianFlow serves as the baseline for comparing trajectory types and scores

performance, particularly in handling occlusions and maintaining robustness across frames, consistent with previous findings [39]. In contrast, other trackers showed significant limitations: Boosting and MIL failed to detect tracking losses, KCF struggled with rapid movements [40], and TLD, although accurate, was computationally intensive [41]. GoTurn required domain-specific training [42]. In contrast, DlibTracker and CamShift were sensitive to speed variations and lighting changes, respectively [43] and [44]. Template Matching also proved unreliable due to sensitivity to appearance changes [45].

Trackers Robustness Analysis

We compared MedianFlow, KCF, and Dlib Tracker across all ten videos. For each tracker we measured (i) track failure rate (percentage of frames after which tracking was lost), (ii) mean frame-to-frame position jitter in centimeters, and (iii) the proportion of lifts where the derived trajectory type or 0–4 score differed from the MedianFlow baseline. Table 5 and Table 6 summarize these results.

Perfect robustness with a 0% failure rate was observed across both MedianFlow initialization methods, making it the benchmark choice for continuous barbell tracking. The Dlib Correlation Tracker showed similarly strong performance, with failure rates of 3.59% (manual) and 0.52% (YOLO). In contrast, KCF demonstrated severe tracking failures–−82.18% with manual ROI and 38.79% with YOLO initialization. We believe the algorithm's reliance on correlation filters appears ill-suited for the rapid motions of lifts, contributing to these results.

Interestingly, under manual initialization, KCF had the lowest jitter (0.070 cm), most likely due to its high failure rate. The tracker often returns static or near-static bounding boxes when tracking is lost, which artificially suppresses frame-to-frame displacement. This may not be a true jitter but an artifact of the tracking failure. MedianFlow and Dlib had comparable jitter values (0.77-−0.81 cm), reflecting genuine barbell motion rather than tracking artifacts. KCF's jitter metric was significantly improved (0.750 cm) with YOLO detections in the tracking pipeline, which provided periodic corrections that re-anchor the tracker to the true object position.

Table 7 Difference between YOLO-based and manual trajectories for each lift

Athlete	Mean error (cm)	Median error (cm)	Max error (cm)	Type changed?	Score changed?
1	1.2	1.1	1.6	No	Yes
2	0.4	0.5	1.0	No	No
3	0.8	0.7	1.1	No	No
4	0.8	0.7	1.1	No	No
5	0.6	0.5	1.1	No	No
6	–	–	–	Yes	Yes
7	0.7	1.0	1.1	No	No
8	0.8	0.7	1.6	No	No
9	1.0	1.1	1.4	No	No
10	0.5	0.5	1.1	No	No

Errors are computed in calibrated image space

When comparing derived trajectory types and kinematic scores against the MedianFlow baseline, KCF showed the weakest agreement—particularly with manual initialization, where 86% of lifts produced different scores, likely due to tracking failures corrupting the trajectory data. YOLO initialization improved KCF's score agreement to 60%, again emphasizing the advantages of periodic re-detection. The Dlib tracker consistently maintained strong agreement (70% score match) across both methods, though it occasionally misclassified trajectory types (30–40% difference rate), likely due to subtle differences in tracked center positions.

Trajectory Classification

Our classification algorithm achieved 70% accuracy, correctly detecting 7 out of 10 trajectories. The misclassifications in the lifts are primarily due to deviations from expected barbell trajectories. In one of the lifts, the barbell did not cross the vertical reference line–a key feature for the Type 1 trajectory type, whereas in the other, it did, leading to confusion between types. Additionally, in one case, the detected trajectory did not align with any predefined type. These discrepancies likely stem from non-standard execution by the athletes, technical errors during the lift, ultimately leading to incorrect classification outcomes.

Agreement Between Automatic and Manual Trajectories

Table 7 depicts a strong agreement between YOLO-based automatic initialization and manual barbell center selection. Across the ten lifts, the mean per-frame position error averaged 0.78 cm (range: 0.4-−1.2 cm), with median errors of 0.79 cm and a maximum instantaneous deviation of 2.0 cm. These variations are unlikely to impact coaching choices or biomechanical interpretation, as they fall well within the standard measurement error of video-based motion capture.

As seen in Table 7, the manually derived trajectory type and those generated with YOLOv11n matched for almost all athletes. The performance score matched in 8 out of 10 cases. For Athlete 6, there was a single trajectory type difference: while manual initialization was unable to identify the trajectory, YOLOv11n successfully tracked the barbell and generated a legitimate Type 4 classification. This example highlights a crucial benefit of automatic detection; YOLOv11n demonstrates more resilience in situations where manual ROI selection might be erratic or prone to human error. Despite sharing the same trajectory types, the score differential for Athlete 1 resulted from a slight variation in the generated X_1 parameter (3.0 cm vs. 2.5 cm) that exceeded the scoring threshold.

Throughout the lift duration, sub-centimeter tracking precision is maintained via the periodic re-detection technique used every 30 frames, which effectively corrects drift. By removing manual involvement, YOLO-based initialization provides a fully automated, repeatable, and more reliable trajectory extraction pipeline.

Kinematic Parameter Extraction

The average height measured by our measurement is 173.33 cm, which is in close accordance with the average height of 175.26 cm [18] for male weight lifters in the USA. The average values of kinematics across 6000 frames are shown in Table 8. Here, we compare the average values of the kinematic parameters with the typical range observed in elite weightlifters [18, 46, 47] to assess measurement efficacy. All these ranges are proportional to the athlete's height. For a valid comparison, measurements are normalized by athlete height. Y_{max} and Y_{catch} are primary vertical measures, with Y_{drop} indicating efficiency. X_{Net}, X_1, X_2, and X_{loop} describe horizontal movement and should be minimized for best techniques. Angle θ describes the bar path and the lifter's mechanics. These ranges provide a robust framework for analyzing and comparing kinematic parameters in Olympic snatch and lift trajectories. For example, efficient lifts (Type I trajectory) typically show minimal X_{Net}, small Y_{drop}, and smooth transitions between phases. We can observe from Table 8 that all parameter averages are within the specified range, ensuring the fidelity of the Computer vision-based measurement.

Table 8 Average values of kinematic parameters and their typical range in Olympic snatch and lift [18, 46, 47] normalized to average athlete height estimated from 10 videos

Parameter	Average value	Typical range %	Typical range (cm)
Y_{max} (cm)	133.00	70 – 85	120 – 145
Y_{catch} (cm)	125.22	60 – 75	100 – 130
Y_{drop} (cm)	07.78	04 – 15	6.5 – 25
X_{net} (cm)	23.61	00 – 10	00 – 17
X_1 (cm)	05.11	02 – 06	03 – 10
θ_1 (degrees)	04.44	05 – 15	–
X_2 (cm)	08.17	02 – 08	03 – 14
X_{loop} (cm)	02.76	02 – 07	03 – 12

The average estimated height is 173.33 cm

Trajectory Detection and Performance Score

The results of 10 videos are summarized in Table 9. For each video, the table compares the trajectory type identified by subject matter experts with the type predicted by our algorithm. It also shows the estimated athlete height using computer vision, along with values for three kinematic parameters. The score is computed by checking whether Y_{max}, X_1, and Y_{drop} fall in the designated range as indicated in Table 8.

Table 9 Classification, barbell kinematic parameters validation, and performance score

Athlete	Type given	Type Pred.	Height cm	Y_{max} cm	X_1 cm	Y_{drop} cm	Score (Cat.)
1	1	**2**	165	129.0	2.5	8.0	0 (Very bad)
2	2	**1**	170	133.5	1.5	9.5	0 (Very bad)
3	3	3	174	137.0	3.5	14	4 (Excellent)
4	3	3	179	139.5	8.0	4.5	4 (Excellent)
5	3	3	185	139.5	**11**	6.0	3 (Good)
6	4	–	–	–	–	–	0 (Very bad)
7	2	2	170	133.5	**3.0**	6.5	3 (Good)
8	1	1	177	139.0	5.0	6.0	4 (Excellent)
9	1	1	178	136.0	3.5	7.0	4 (Excellent)
10	1	1	162	126.0	5.5	8.5	4 (Excellent)

The boldface indicates incorrect classification or a parameter not in the range. Cat. indicates the category of the score

Table 10 Peak force, peak vertical velocity, and peak power for each athlete, grouped by performance score category

Athlete	Peak force (N)	Peak velocity (m/s)	Peak power (W)	Mass (kg)
1	750.81	2.21	1578.72	60
2	800.57	2.13	1563.34	56
3	857.85	2.01	1426.14	65
4	1016.67	1.98	1946.55	81
5	1191.42	2.10	2377.30	100
6	–	–	–	–
7	1455.43	2.43	3204.29	95
8	1461.21	2.13	2735.38	100
9	1412.59	2.26	2956.57	106
10	1626.94	2.01	3060.94	128

From Table 9, we observe that for athletes 1, 2, and 6, the trajectory could not be correctly classified; therefore, they were assigned a 0 score or a very poor category. We can see that most athletes exhibited good vertical barbell displacement, with Y_{max} values that closely matched their respective heights, ranging from 120 to 145 cm. This suggested that they could generate sufficient vertical force during the lift. X_1, representing the initial horizontal position, was within the ideal range (3 - 10 cm) for most lifts, except for athletes 5 and 7, indicating a proper starting setup for them. For athletes 5 and 7, the score is 3, and a Good category is generated because X_1 falls outside the ideal range. Similarly, the bar drop (Y_{drop}) was in the expected range of 6.5 - 25 cm for efficient catch mechanics in most cases. Overall, athletes 3, 4, 8, 9, and 10 achieved a score of 4, indicating excellent category lifts, as they consistently demonstrated Y_{max}, controlled X_1 displacement, and optimal bar drop values.

Biomechanical Relationship: Force, Power, Velocity, and Lift Quality

Table 10 presents the peak velocity, force, and power for each athlete. Understanding how these three variables influence lift quality is essential. Peak power represents the product of force and velocity ($P = F \times v$), and achieving a successful snatch requires not only sufficient force production but also a minimum barbell velocity threshold.

Our results clearly demonstrate the significance of velocity. While higher force production increases peak power, excessive force at the expense of velocity compromises lift success. For instance, Athlete 7 generated the highest peak velocity (2.43 m/s) and achieved a peak power of 3204.29 W with a 95 kg barbell, earning a "Good" rating. In contrast, Athlete 4 produced a lower peak velocity (1.98 m/s) but achieved an "Excellent" rating, suggesting that the optimal balance between force and velocity was maintained throughout the lift. These findings imply that lift quality is not solely determined by raw force output; rather, high peak power and effective technique result from a harmonious combination of force and velocity.

Athletes 1 and 2, despite producing adequate velocities (2.21 m/s and 2.13 m/s respectively), received "Very Bad" scores due to trajectory classification failures. This illustrates the need for both proper technical execution and physical output metrics; even if an athlete produces enough force and velocity, the lift may still fail if the barbell path deviates from ideal patterns. Comparing Athletes 5 and 10, both achieved similar peak velocities (2.10 m/s and 2.01 m/s), but Athlete 10, using a heavier 128 kg barbell, produced higher peak force (1626.94 N vs. 1191.42 N) and power (3060.94 W vs. 2377.30 W). This demonstrates that heavier loads require greater force while maintaining the velocity threshold required for a successful lift.

These results highlight the importance of velocity as a mediating factor between force and power. Regardless of the lifter's strength, the lift will fail if the barbell velocity drops below the threshold needed to complete the catch phase. Conversely, high peak power output and successful lift execution are made possible by an ideal balance of force and velocity, ensuring neither is sacrificed for the other.

Table 11 Effect of scale perturbation on kinematic ranges and score

Perturbation	Flips in $Y_{\max}$ range	Flips in X_1 /Y_{drop} range	Lifts with score change
$\pm 5\%$	2	2	3
$\pm 10\%$	4	2	5

Pixel-Centimeter Calibration Robustness of Performance Score

Table 11 summarises the effect of perturbing the pixel-to-centimetre scale factor by $\pm 5\%$ and $\pm 10\%$. At the $\pm 5\%$ level, 2 of 10 lifts experienced a flip in the in-range status of $Y_{\max}$, while X_1/Y_{drop} flipped in 2 lifts, resulting in 3 lifts with an overall score change. At the $\pm 10\%$ level, $Y_{\max}$ flips increased to 4 lifts and score changes to 5 lifts. Upon closer examination, every lift that was impacted had at least one kinematic parameter close to a score threshold border. There was no change in score for the remaining 7 lifts at $\pm 5\%$ (70%) and 5 lifts at $\pm 10\%$ (50%), whose characteristics were either obviously beyond the allowed range or well inside it. Any threshold-based scoring system is mathematically expected to exhibit this behavior. These findings imply that, in reality, the scoring system is reliable for most lifts, with calibration-induced variability mainly affecting borderline situations where little variations in measurement could reasonably change the biomechanical interpretation.

(a) (i) (b) (ii) (c) (iii)

Fig. 7 Tracking challenges: i. Occlusion due to the background person, ii. Video taken from an angle, iii. The barbell is exiting the camera plane

Limitations of the Proposed Approach

The reliability of the proposed approach is based on certain assumptions. One major limitation is the need to manually draw bounding box annotations around the barbell. Some vision-related challenges are shown in Fig. 7. Occlusions from background objects led to tracking failures or inaccuracies. Additionally, the method assumes that the camera is laterally aligned with the athlete performing the lift. When the videos are captured from a high angle (20 degrees or more), this assumption breaks down. This would require preprocessing the videos to correct the affine transformation. Furthermore, tracking continuity was lost if the barbell moved out of the camera frame due to an improper field of view.

Another major issue arose when another athlete performed a different movement behind the main subject, causing the tracker to lock onto the background motion instead of the barbell. Lastly, an excessively high frame rate introduced motion blur and unnecessary frame redundancy, making it challenging to extract precise kinematic variables of the barbell. Since the approach relies on pixel-level measurements to classify trajectory patterns and calculate derived metrics, the resulting perspective distortions lead to improper trajectory classification and reduce the interpretability of the results. The performance score could be more discriminative with the addition of features such as velocity and total power during the lifts. These challenges underscore the importance of meticulous camera placement, judicious frame rate selection, and refined tracking methods to improve the accuracy of motion analysis.

Additionally, inter-individual anthropometric differences influence optimal barbell trajectories and may lead to stylistic variations that are not fully captured by a unified scoring framework. The two-dimensional trajectory representation further limits assessment of out-of-plane motion, which may be relevant for certain lifting styles. These constraints reflect the inherent trade-offs between ecological validity and measurement precision in video-based analysis systems.

Conclusion and Future Work

This updated study improves on the previously proposed framework by making it a more comprehensive system for analyzing barbell trajectories and assessing biomechanical performance. The research now clearly situates trajectory elements within established phase models of the snatch, explaining how the spatial kinematics of the barbell relate to technical goals and potential injury processes during the first pull, transition, second pull, and catch phases. By incorporating calculations for velocity and power, and linking them to lift quality, the evaluation extends beyond positioning measures to provide a more comprehensive view of force output and mechanical effectiveness.

The pipeline has been improved from start to finish in terms of methodology. Automatic YOLO-based barbell recognition takes the place of manual initialization. A tracking ablation and multi-tracker robustness analysis (like MedianFlow or KCF) measures how different tracking choices change barbell trajectories, derived kinematic variables, and the final 0–4 score. Calibration sensitivity experiments, along with direct assessments of noise in Y_{max}, X_1, and Y_{drop}, demonstrate that the scoring framework remains predominantly stable despite realistic inaccuracies in the pixel-to-centimeter conversion and tracking jitter, thereby validating the numerical reliability of the proposed metric for practical application.

In an analytical way, the work now examines the differences between human and automated trajectories, how these differences affect kinematic estimations, and shows that automated initialization seldom alters the trajectory type or performance category for high-quality lateral views. The additional comparative analysis of tracking algorithms and the calibration robustness of the performance score provides

a clear picture of where the system performs well and where it doesn't, especially when the camera is at an angle or the video quality is poor, which is often the case in real-world situations. This research collectively advances the contribution from a proof-of-concept classifier to a verified measurement instrument with well-defined parameters.

There are still important limits, though. The research is still based on a small number of competition lifts, and the current two-dimensional model can't capture out-of-plane variations that may be important for some lifters. Because people have different body types and style preferences, a single rule-based scoring system can't fully show all technically possible paths. This shows that more work is needed on customized or learning-based models. To make the scoring thresholds more accurate and transform the framework from a snatch-only analysis tool into a generalizable tool for all Olympic lifts, it will be essential to incorporate more data, utilize richer three-dimensional or multi-view information when possible, and combine expert ratings on a large scale. More so, the YOLO detector is trained on labeled frames extracted from the same ten competition videos used for the tracking evaluation. While this perfectly demonstrates the system's capability to automate tracking in a known environment, future work would evaluate the YOLO pipeline on completely unseen video sets to fully confirm generalization. We note that perspective distortion from oblique angles reduces detection accuracy; therefore, we will leverage standard homography or perspective transform techniques as a viable preprocessing step to auto-correct these angles. This will move the work toward personalized or learning-based scoring to improve robustness.

Acknowledgements The authors thank the weightlifters and coaching staff for their cooperation and participation in this study. We also thank Varun Deliwala for the initial layout of the framework and approach.

Author Contributions Dhairya Shah: Conceptualization, literature review, methodology; writing – original draft. Hetav Raval: Conceptualisation, literature review, writing, automation of trajectory, uncertainty analysis, preparation of figures and tables; manuscript formatting; Eva Maddox: Data curation, Statistical analysis (RMSE/MAE/MSE, robustness checks, external validation). Tolga Kaya: interpretation of results, editing, and investigation. Christopher Taber: Domain expertise (sports science/strength, conditioning); protocol design; interpretation for practice; writing – review, editing. Mehul S Raval: Predictive modeling and experiments, formal analysis; visualization, writing – review, editing.

Funding Not Applicable

Data Availability Due to the personal nature of the data, it cannot be publicly released. However, an anonymized sample dataset is available on the GitHub repository (a link can be provided upon acceptance).

Materials Availability Not Applicable.

Code Availability Code will be available on the GitHub repository upon paper acceptance.

Declarations

Conflict of interest On behalf of all authors, the corresponding author states that there is no Conflict of interest.

Ethical Approval and Consent to Participate Before participation, all participants received detailed explanations of the study procedures and provided informed consent with Institutional review board approval number 170720a at Sacred Heart University, USA.

Consent for Publication Not Applicable

References

1. Weightlifting U. The Lifts. Accessed: 2025. https://www.usaweightlifting.org/weightlifting101/the-lifts
2. Federation IW. What Are the 2 Olympic Lifts? Accessed: 2025. https://iwf.sport/2017/11/27/2-olympic-weightlifting-lifts/
3. Federation IW: IWF Technical and Competition Rules & Regulations. https://iwf.sport/technical-and-competition-rules/. Accessed: 2025-04-19 2024
4. Federation IW. Bodyweight Categories – IWF. https://iwf.sport/bodyweight-categories/. Accessed: 2025-04-19 2024
5. Garhammer J. A review of power output studies of olympic and powerlifting: methodology, performance prediction, and comparative analysis. J Strength Cond Res. 1993;7(2):76–89.
6. contributors W.:Snatch (weightlifting). https://en.wikipedia.org/wiki/Snatch_(weightlifting). Accessed: 2025-04-19 2024
7. contributors W. Clean and jerk. https://en.wikipedia.org/wiki/Clean_and_jerk. Accessed: 2025-04-19 2024
8. Federation IW. Specifications for competition equipment. https://iwf.sport/weightlifting_equipment. Accessed: 2025-04-19 2023
9. International Weightlifting Federation: Technical and Competition Rules & Regulations. Online; Accessed April 4, 2025. https://iwf.sport/wp-content/uploads/downloads/2020/03/IWF_TCRR_2020.pdf 2020
10. Strength V. Absolute training Kg bumper plates & barbell set. Online; Accessed April 4, 2025. https://www.vulcanstrength.com/Absolute-Training-Kg-Bumper-Plates-Barbell-Set-p/v-atkgbarbump160.htm2025
11. Gourgoulis V, Aggeloussis N, Kalivas V, Antoniou P, Mavromatis G. Biomechanical differences of snatch technique between elite male and female weightlifters. J Sports Med Phys Fitness. 2009;49(1):1–7.
12. Huebner M, Perotto A, Suchomel TJ. Biomechanics of olympic weightlifting: a review. Strength Cond J. 2021;43(3):56–69.
13. Baumann W, Gross V, Quade K, Galbierz P, Schwirtz A. The snatch technique of world class weightlifters at the 1985 world championships. Int J Sport Biomech. 1988;4(1):68–89.
14. Garhammer J. A review of power output studies of olympic and powerlifting: methodology, performance prediction, and evaluation tests. J Strength Cond Res. 1991;5(2):89–102.
15. Thiele F, Paternoster F, Hummel C, Stöcker F, Holzer D. Assessment of the accuracy of a deep learning algorithm-and video-based motion capture system in estimating snatch kinematics. Int J Exerc Sci. 2024;17(1):1629.
16. Gourgoulis V, Aggeloussis N, Garas A, Mavromatis G. Snatch lift kinematics and bar energetics in male adolescent and adult weightlifters. J Sports Med Phys Fitness. 2000;40(2):126–31.

17. Chavda S, Hill M, Martin S, Swisher A, Haff GG, Turner AN. Weightlifting: An applied method of technical analysis. Strength Cond J. 2021;43(4):32–42.
18. Cunanan AJ, Hornsby WG, South MA, Ushakova KP, Mizuguchi S, Sato K, Pierce KC, Stone MH. (2020) Survey of barbell trajectory and kinematics of the snatch lift from the 2015 world and 2017 pan-american weightlifting championships. Sports **8**(9) https://doi.org/10.3390/sports8090118
19. Garhammer J. A review of power output studies of olympic and powerlifting: methodology, performance prediction, and evaluation tests. J Strength Cond Res. 1993;7(2):76–89.
20. Dæhlin TE, Krosshaug T, Chiu LZF. Enhancing digital video analysis of bar kinematics in weightlifting: a case study. J Strength Cond Res. 2017;31(6):1592–600. https://doi.org/10.1519/JSC.0000000000001618.
21. Enoka RM. Neuromechanics of Human Movement. Human Kinetics, ??? 2008
22. TENDO Unit Overview. https://www.tendosport.com/products/tendo-unit/overview/. Accessed: 2025-04-30 (2025)
23. GymAware RS (LPT) - Gold Standard VBT device. https://gymaware.com/gymaware-rs/. Accessed: 2025-04-30 (2025)
24. Weakley JJS, Mann B, Banyard HG, McLaren SJ, Scott T, Garcia-Ramos A. Comparison of velocity-based and percentage-based training methods for improving strength and power in collegiate athletes. Int J Sports Physiol Perform. 2021;16(4):516–23. https://doi.org/10.1123/ijspp.2020-0444.
25. Balsalobre-Fernández C, Kuzdub M, Poveda-Ortiz P, Campo-Vecino JD. Validity and reliability of the push wearable device to measure movement velocity during the back squat exercise. J Strength Cond Res. 2017;31(9):2610–7. https://doi.org/10.1519/JSC.0000000000001742.
26. Chiu LZF, Schilling BK. A kinematic analysis of a weightlifting exercise using mathematical modeling. Strength Cond J. 2005;27(1):42–51.
27. Picerno P. Wearable inertial sensors for human movement analysis: a five-year update. J Biomed Sci Eng. 2017;10(8):147–56. https://doi.org/10.4236/jbise.2017.108012.
28. Colyer SL, Evans M, Cosker DP, Salo AIT. A review of the evolution of vision-based motion analysis and the integration of advanced computer vision methods towards developing a markerless system. Sports Med Open. 2018;4(1):24. https://doi.org/10.1186/s40798-018-0139-y.
29. Balsalobre-Fernández C, Cuspinera E, Campo-Vecino JD, Romero-Moraleda B. Automatic identification of vertical jumps using smartphone video analysis: a reliability and validity study. J Strength Cond Res. 2020;34(10):2953–9. https://doi.org/10.1519/JSC.0000000000003734.
30. Mathis A, Warren RA, Uchida T, Suleiman A, Mathis MW. Deep learning tools for the measurement of animal behavior in neuroscience. Curr Opinion Neurobiol 2020;60:1–11 https://doi.org/10.1016/j.conb.2019.10.008
31. Shah D, Taber C, Kaya T, Maddox E, Raval MS. Barbell trajectory tracking for performance analysis during snatch movement in weightlifting. In: International Sports Analytics Conference and Exhibition, 2025:218–234 . Springer
32. GoPro: GoPro HERO9 Black – more everything. https://gopro.com/en/us/news/hero9-black-launch. Accessed: 2025-04-19 2020
33. OpenCV Team: cv::TrackerMedianFlow Class Reference. https://docs.opencv.org/3.4/d7/d86/classcv_1_1TrackerMedianFlow.html. Accessed: 2025-04-02 2021
34. Jocher G, Qiu J, Chaurasia A. Ultralytics YOLO11. GitHub repository 2024
35. Bradski G, Kaehler A. Opencv. Dr Dobb's journal of software tools. 2000;3(2):1–81.
36. Whittlesey S. Biomechanics of Sport and Exercise, 3rd edn. Human Kinetics, ??? 2017
37. Isaka T, Okada J, Funato K. Kinematics analysis of the barbell during the snatch movement of elite asian weightlifters. J Appl Biomech. 1996;12(4):508–16.
38. Baehrle RE, Earle RW. Fitness and Wellness. McGraw-Hill Education, ??? 2000
39. Varfolomieiev A, Lysenko O. An improved algorithm of median flow for visual object tracking and its implementation on arm platform. J Real-Time Image Proc. 2013;11(3):527–34. https://doi.org/10.1007/s11554-013-0354-1.
40. Henriques JF, Caseiro R, Martins P, Batista J. High-speed tracking with kernelized correlation filters. IEEE Trans Pattern Anal Mach Intell. 2015;37(3):583–96. https://doi.org/10.1109/TPAMI.2014.2345390.
41. Kalal Z, Mikolajczyk K, Matas J. Tracking-learning-detection. IEEE Trans Pattern Anal Mach Intell. 2012;34(7):1409–22. https://doi.org/10.1109/TPAMI.2011.239.
42. Held D, Thrun S, Savarese S. Learning to track at 100 fps with deep regression networks. In: European Conference on Computer Vision, Springer, ??? 2016:749–765 https://doi.org/10.1007/978-3-319-46448-0_45
43. King DE. Dlib-ml: a machine learning toolkit. J Mach Learn Res. 2009;10:1755–8.
44. Bradski GR. Computer vision face tracking for use in a perceptual user interface. Intel Technol J. 1998;2(2):1–15.
45. Brunelli R. Template Matching Techniques in Computer Vision: Theory and Practice. John Wiley & Sons, ??? 2009
46. Harbili E, Alptekin A. Comparative kinematic analysis of the snatch lifts in elite male adolescent weightlifters. J Sports Sci Med. 2014;13(2):417–22.
47. Nagatani T, Haff GG, Guppy SN, Poon W, Kendall KL. Effect of different set configurations on barbell trajectories during the power snatch. Int J Sports Sci Coach. 2022;18(5):1594–604. https://doi.org/10.1177/17479541221116965. (Original work published 2023).